



# Voltammetric lidocaine sensor by using a glassy carbon electrode modified with porous carbon prepared from a MOF, and with a molecularly imprinted polymer

Junjie Zhang<sup>1</sup> · Jiang Liu<sup>2</sup> · Yang Zhang<sup>2</sup> · Feng Yu<sup>3</sup> · Fu Wang<sup>4</sup> · Zhengchun Peng<sup>5</sup> · Yingchun Li<sup>2</sup>

Received: 28 July 2017 / Accepted: 9 November 2017 / Published online: 26 December 2017  
© Springer-Verlag GmbH Austria, part of Springer Nature 2017

## Abstract

The work describes a hybrid electrochemical sensor for highly sensitive detection of the anesthetic lidocaine (LID). Porous carbon (PC) was synthesized from an isoreticular metal-organic framework-8 (IRMOF-8) and drop cast onto a glassy carbon electrode (GCE). A layer of a molecularly imprinted polymer (MIP) layer was then fabricated in situ on the modified GCE by electro-polymerization, with LID acting as the template and resorcinol as the functional monomer. Hexacyanoferrate is used as an electrochemical probe. The electrical signal (typically acquired at 0.335 V vs. SCE) increases linearly in the 0.2 pM to 8 nM LID concentration range, with a remarkable 67 fM detection limit (at an S/N ratio of 3). The sensor is stable and selective. Eventually, rapid and accurate detection of LID in spiked real samples was successfully realized.

**Keywords** MOF derived carbon · Electrochemical sensor · Cyclic voltammetry · Trace measurement · Scanning electron microscopy · X-ray photoelectron spectroscopy · Raman spectra · Brunauer-Emmett-Teller · Nanoporous material · Hexacyanoferrate

**Electronic supplementary material** The online version of this article (<https://doi.org/10.1007/s00604-017-2551-2>) contains supplementary material, which is available to authorized users.

✉ Zhengchun Peng  
zcpeng@szu.edu.cn

✉ Yingchun Li  
liyinchun@hit.edu.cn

<sup>1</sup> Key Laboratory of Xinjiang Phytomedicine Resource and Utilization, Ministry of Education, Shihezi University, Shihezi 832000, China

<sup>2</sup> College of Science, Harbin Institute of Technology, Shenzhen 518055, China

<sup>3</sup> Key Laboratory for Green Processing of Chemical Engineering of Xinjiang Bingtuan, School of Chemistry and Chemical Engineering, Shihezi University, Shihezi 832003, China

<sup>4</sup> Laboratory of Environmental Science and Technology, The Xinjiang Technical Institute of Physics and Chemistry; Key Laboratory of Functional Materials and Devices for Special Environments, Chinese Academy of Sciences, Urumqi 830011, China

<sup>5</sup> College of Optoelectronic Engineering, Shenzhen University, Shenzhen 518060, China

## Introduction

Lidocaine (LID) is a local anesthetic and antiarrhythmic drug [1]. It is also the preferred drug in the treatment of myocardial infarction ventricular premature beats and ventricular tachycardia [2]. However, excessive blood concentration of LID can cause cardiovascular and central nervous system diseases [3]. What's more, LID is currently being illegally added into cosmetics to reduce skin damage from sun exposure [4]. Therefore, it is necessary to detect LID in biological fluids and cosmetic products. The most commonly applied methods of LID detection include high performance liquid chromatography [5, 6] (HPLC), gas chromatography-mass spectrometry [7, 8] (GC-MS), etc. However, large instrument-based approaches have some shortcomings such as use of environmentally unfriendly reagents, long working time, tedious pretreatment and high cost [9]. Compared with these tools, electrochemical method can largely reduce energy and reagent consumption, simplify pretreatment and shorten detection time [10, 11]. Additionally, electrochemical sensors feature the advantages of easy preparation and operation, low detection limit

and high sensitivity, allowing for rapid and on-the-spot monitoring of trace analytes [12].

Some direct electrochemical approaches for monitoring LID have been developed [13–16]. However, selectivity is an inherent bottleneck for sensor-based detection, which limits its application since existence of various interferants is a ubiquitous phenomenon in real sample analysis [17]. In order to solve this problem, molecularly imprinted polymer (MIP) can be introduced as a very proper target molecule recognizer [18, 19]. Moreover, together with applying electrochemical probes as electrical signal indicators, the MIP-based sensor does not rely on analyte inherent electrochemical activity and thus theoretically can detect any chemicals [12, 20].

In addition, studies also point out that sensor substrate is an important factor impacting sensitivity and selectivity [21, 22]. In this respect, various modifiers have been used to decorate electrodes to improve sensing performance. Among them, porous carbon, as conductive nanomaterial, is suitable modifier due to its large surface area, good stability, mass productivity and low cost [23, 24]. There is a rapidly growing attention on metal organic framework (MOF) derived porous carbon, in which MOF is used as a precursor due to its excellent performance like diverse structure and tunable property [25, 26]. In order to obtain porous carbon with less aggregational fragments and better dispersity, further treatment is necessary. N-methyl-2-pyrrolidone (NMP) has been adopted in dispersing two-dimensional materials due to its nonvolatility, low toxicity and high viscosity [27], which is an ideal option in obtaining fully dispersed and stabilized porous carbon materials via tender and relatively safe operation [21]. What's more, to the best of our knowledge, there is no report on combination of MOF derived porous carbon (PC) with MIP for electrochemical sensor application.

In this work, we constructed a novel electrochemical method based on MIP and PC hybrid sensor for determination of LID. PC exhibited good dispersity, huge surface area and large pore volume, therefore enhancing sensor conductivity and providing ample loading surface for MIP immobilization. The new electrochemical sensing platform combined MIP and PC, ensuring high sensitive and selective determination of LID. Relevant parameters influencing the sensing performance were carefully optimized and the resulting sensor was successfully used for LID detection in blood samples.

## Experimental

### Materials and apparatus

LID, bupivacaine hydrochloride (BC), dopamine and N,N-dimethylformamide (DMF) were bought from Shanghai Adamas Reagent Co. Ltd. (Shanghai, China; [www.adamas-beta.com](http://www.adamas-beta.com)). Phenylenediamine, resorcinol and *o*-

aminophenol were purchased from Shanghai Aladdin Co. Ltd. (Shanghai, China; [www.aladdin-e.com](http://www.aladdin-e.com)). Prilocaine (PC), mepivacaine (MC) and NMP were purchased from Sigma-Aldrich Co. Ltd. (Shanghai, China; [www.sigmaaldrich.com](http://www.sigmaaldrich.com)). Rat blood samples were obtained from laboratory animal center of Shihezi University. Reagents and materials, such as  $K_3[Fe(CN)_6]$ ,  $K_4[Fe(CN)_6]$ , glucose, NaCl,  $CHCl_3$ ,  $NH_4Cl$ ,  $H_2SO_4$ ,  $KNO_3$ ,  $HNO_3$ , methanol, NaOH, acetonitrile and phosphate buffer (PB,  $KH_2PO_4$  and  $K_2HPO_4$ ) were of the analytical level. All solutions were prepared using double distilled water.

Electrochemical measurements were carried out on a CHI 660E Electrochemical Workstation (ChenHua Instruments Co. Ltd., Shanghai, China; [www.chinstr.com](http://www.chinstr.com)) connected to a PC at room temperature. A typical three-electrode system was employed with a platinum wire (0.5 mm in diameter and 34 mm in length) as the counter electrode, a saturated calomel electrode (SCE) as the reference electrode. The working electrode was a bare or modified glassy carbon electrode (GCE, 4 mm in diameter). All potentials given in this paper were referred to SCE.

Surface morphology of the employed materials was characterized using a Zeiss Supra55VP scanning electron microscope (SEM) operating at 20 kV. A centrifuge (Anke TGL-16G, Shanghai, China; [www.shanting17.com](http://www.shanting17.com)) was used in pretreatment of biological samples. HPLC was performed with a Shimadzu (Japan) system comprising of LC-10A pumps and an SPD-10A UV-detector. Chromatographic conditions were as follows: separation was performed on a WondaSil  $C_{18}$  column (150 mm  $\times$  4.6 mm i.d., 5 mm) which was purchased from Dalian Elite Analytical Instruments Co. Ltd. (Dalian, China; [www.elitehplc.com](http://www.elitehplc.com)). Mobile phase was mixture of acetonitrile and PB (pH = 3) at the volumetric ratio of (12:88). The flow rate was 1.0 mL  $min^{-1}$  and the detection wavelength was 210 nm.

### Preparation of PC

IRMOF-8 was synthesized via solvothermal method. Briefly, 1.19 g  $Zn(NO_3)_2 \cdot 6H_2O$  and 0.43 g 2,6-naphthalenedicarboxylic acid were dissolved in 40 mL DMF to get a clear solution. The solution was then transferred to a 50 mL Teflon vessel in an autoclave which was placed in an oven and kept at 120 °C for 20 h. After reaction, the autoclave was cooled to room temperature. The mixture was filtered and washed three times with DMF and  $CHCl_3$  successively, followed by full immersion in fresh  $CHCl_3$  and drying at 120 °C for 2 h to get IRMOF-8 crystals. And then about 1 g IRMOF-8 was heated at 1000 °C for 5 h under nitrogen environment. Through this carbonization process, derived porous carbon was prepared. Afterwards, the porous carbon (80 mg) was dispersed in 80 mL of NMP, and then transferred to 100 mL reagent bottle. The sealed bottle was sonicated in a

KQ-5200 ultrasonicator for 24 h (40 kHz, 100 W). After 2 h quiescence, the supernatant was filtered through a 0.22  $\mu\text{m}$  membrane filter, washed with ethanol, and dried at 60  $^{\circ}\text{C}$  for 12 h to obtain PC.

### Fabrication of MIP/PC film modified sensor

GCE was polished successively with 0.30 and 0.05 mm alumina powder, and then cleaned with distilled water. 1 mg PC was suspended in 1 mL DMF at the ratio of 1 mg mL<sup>-1</sup>. 15  $\mu\text{L}$  PC-DMF suspension was dropped onto GCE surface and dried under infrared lamp for fabrication of PC/GCE.

MIP was synthesized via electro-polymerization in phosphate buffer containing  $2 \times 10^{-3}$  M resorcinol (as functional monomer) and  $1 \times 10^{-3}$  M LID (as template) by cyclic voltammetry (CV) carried out from 0 V to 1.0 V (vs. SCE) for 60 cycles at a scan rate of 50 mV s<sup>-1</sup>. After polymerization, the polymer film-covered PC/GCE was immersed in 0.1 M NaOH in order to extract the embedded LID by cyclic potential sweeping from -0.5 V to 0.5 V for 5 cycles until a couple of obvious and stable oxidation peaks were showed in probe solution (5 mM [Fe(CN)<sub>6</sub>]<sup>3-/4-</sup> and 0.1 M KNO<sub>3</sub>). The schematic preparation of MIP/PC/GCE is illustrated in Fig. 1.

For comparison, non-imprinted polymer (NIP) modified PC electrode (NIP/PC/GCE) was fabricated in the similar way except the participation of LID.

### Electrochemical measurements

CV served as a method to evaluate electrochemical behavior of different electrodes in probe solution. Performances of differently modified sensors were evaluated by comparing the change of peak current intensity ( $\Delta I$ ) before and after binding with LID.

The determination procedure is as follows: a sensor was immersed in probe solution and its cyclic voltammetric curve was recorded. After that, the sensor was incubated in solution containing certain amount of analyte for 10 min, followed by rinsing with water to remove loosely sorbed substances. The sensor was measured again via CV carried out from -0.2 V to 0.6 V (vs. SCE) for 3 cycles at a scan rate of 50 mV s<sup>-1</sup> to record its electrochemical response after exposure to analyte. The peak currents shift ( $\Delta I$ ) was calculated from the change of oxidation peak currents before and after binding with LID. After each analysis, sensor was recovered by CV scanning in the range of -0.5 ~ +0.5 V in 0.1 M NaOH for 5 cycles. Electrochemical impedance spectroscopy (EIS) experiments were carried out in solution containing 5 mM [Fe(CN)<sub>6</sub>]<sup>3-/4-</sup> and 0.1 M KCl within a frequency range from 0.01 Hz to 100 kHz.

### Detection of LID in biological samples

In order to explore the performance and practicability of the method in analyzing real samples, a certain amount of LID standard ( $2.0, 4.0, 6.0 \times 10^{-12}$  M) was mixed into rabbit blood samples for spiked recovery experiment. 1 mL serum was prepared by centrifugation of blood sample at 4000 rpm for 10 min, and then methanol was added into the serum at volumetric ratio of 1 : 1. The mixture was centrifuged again at 4000 rpm for 10 min to precipitate protein, and the final supernatant was used for LID detection.

## Results and discussion

### Choice of materials

Modification of sensor is vital for sensitivity and selectivity. In this respect, various modifiers have been used to decorate electrodes to improve sensing performance. Among them, porous carbon at nano-scale, as conductive material, is suitable agent due to its hierarchical porous architecture, large surface area, good stability and sufficient availability [28]. In addition, MOFs own high carbon contents, and therefore are excellent carbon precursors. The central metal of IRMOF-8 is zinc. Compared with the MOFs whose central ion is nickel, copper or chromium [29], IRMOF-8 can be prepared in more gentle reaction condition with lower cost [25]. Therefore, IRMOF-8 is chosen as the precursor for preparing porous carbon. The subsequent NMP treatment of the porous carbon further elevates the surface to volume area of the material, in favor of obtaining very sensitive electrochemical sensors.

### Preparation and characterization of LID-MIP/PC/GCE electrode

Preparation of MIP/PC/GCE was optimized and the details are elaborated in the Supporting Information file. The optimal sensing performance was obtained when resorcinol was used as the monomer, the pH value of polymerization solution was 7.5 (Fig. S1) and the ratio of template to monomer was 1 : 2 (Fig. S2). The subsequent experiments were carried out under the optimum condition. Surface morphology of the prepared materials was characterized by SEM. As shown in Fig. 2a, PC exhibits thin hierarchical fragments at nanoscale with mesopores and macropores, and the pore size ranges from 50 nm to 250 nm. After modification of PC via electro-polymerization in the presence of monomer and LID, the surface of PC gets rougher and the width of pore size is reduced (Fig. 2b) by around 20% (pore size range is 40 ~ 200 nm). These might be side notes implying successful preparation of MIP membrane which covers the surface of PC evenly. Subsequent extraction of LID molecules from the polymeric

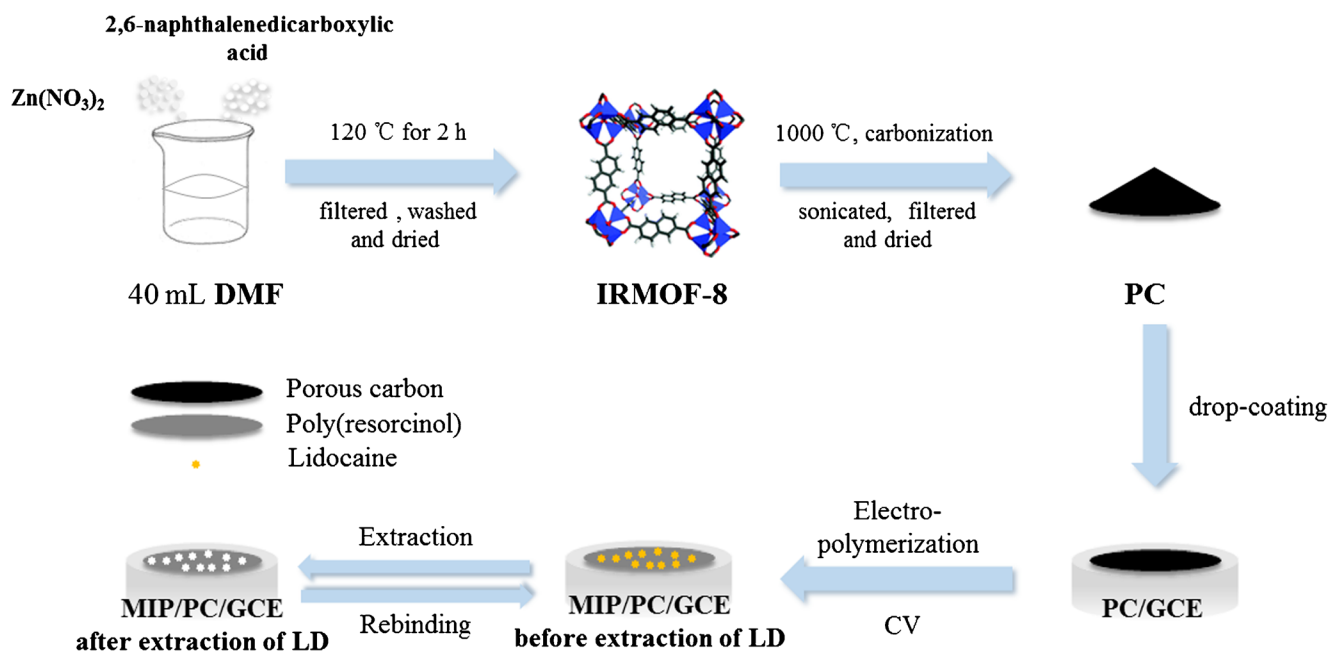


Fig. 1 Schematic of the preparation of MIP/PC/GCE

network causes little change in the morphology of MIP–PC hybrid (Fig. 2c), indicating that elution operation does not damage the structure of MIP film.

X-Ray photoelectron spectroscopy (XPS) was performed to determine the elemental content of PC (Fig. 2d). The XPS spectrum of PC possesses two peaks centered at 284.8 eV and 527.6 eV, corresponding to C 1s and O 1s. The magnified C 1s spectrum of PC (inset in Fig. 2d) can be deconvoluted into two peaks (284.7 eV and 289.4 eV), which were assigned to  $sp^2$  hybridized C–C and O–C=O, respectively [30]. The oxygen mainly arises from the thermally stable groups in carbon instead of oxygen or water absorbed on the carbon surface [31]. The carbon forms in PC were confirmed using Raman

spectroscopy (Fig. 2e). It shows well-defined bands at 1352 and 1591  $cm^{-1}$ , which correspond to disordered structures of carbon materials (D band) and graphitic  $sp^2$  carbons (G band), respectively [25]. The D to G band intensity ratio ( $I_D / I_G$ ) was calculated to be 0.98, indicating that PC has a low graphitization degree. The porous structure of PC was evaluated by nitrogen adsorption-desorption analysis (Fig. 2f). The Brunauer-Emmett-Teller (BET) surface area and the total volume were calculated to be 1416.25  $m^2 g^{-1}$  and 1.66  $cm^3 g^{-1}$ , respectively. The adsorbed volume in the adsorption isotherm gradually increased in the range of  $P / P_0 = 0.4 \sim 0.95$ , indicating formation of pores with micropores and mesopores [28, 32]. In comparison with some reported MOF

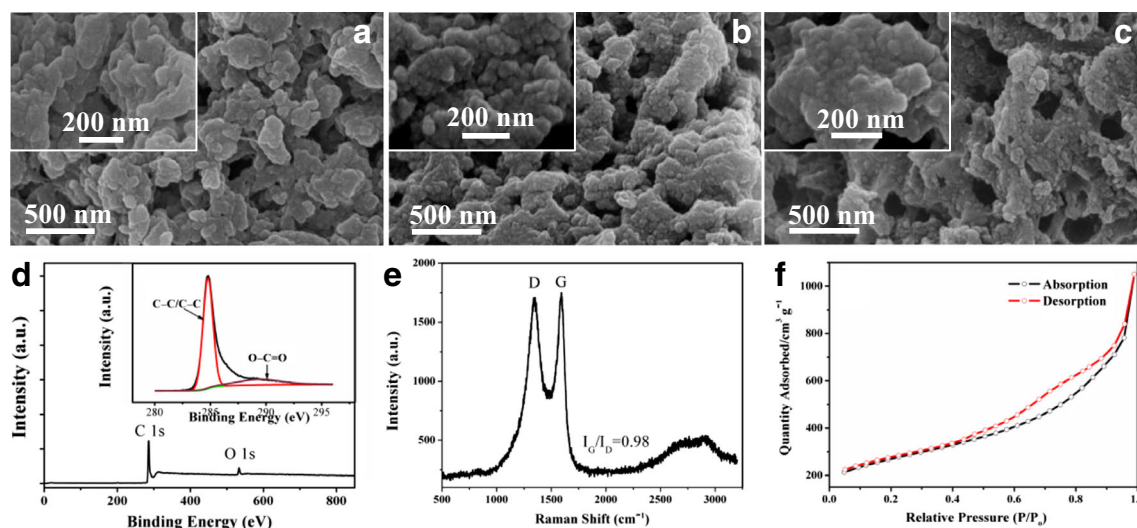


Fig. 2 SEM micrographs of PC (a), MIP/PC before (b) and after (c) extraction of LID; XPS spectrum (inset: high-resolution C 1 s spectrum) (d), Raman spectrum (e) and Nitrogen adsorption-desorption isotherm of PC (f)

derived porous carbon materials, PC in our work features huge surface area and the largest total pore volume (Table S1).

Electrochemical behavior of the stepwise modification procedure at electrode surface was studied in probe solution by CV (Fig. S3A) and EIS (Fig. S3B). Characteristic redox peak currents of  $[\text{Fe}(\text{CN})_6]^{3-/4-}$  got enlarged after PC modification, indicating that PC significantly enhanced signal due to its large conductive surface area. After electro-polymerization of functional monomer and LID, the redox peaks of  $[\text{Fe}(\text{CN})_6]^{3-/4-}$  disappeared. This can be attributed to the formation of densely covered non-conductive polymeric film, which inhibited the access of probe ions to the electrode surface. After template extraction, reappearance of peaks can be explained by the fact that the left cavities due to removal of LID provided doors for the probe ions to reach the electrolyte/electrode interface. Incubation of sensor in LID solution let LID molecules occupy the imprinting sites and hindered the electron transport of  $[\text{Fe}(\text{CN})_6]^{3-/4-}$ , therefore causing reduced current value. EIS tracked the impedance changes at electrode surface, of which the results are in consistent with CV. More detailed descriptions can be found in [electronic supplementary material](#).

For investigating the role of MIP in sensing response, NIP/PC/GCE was prepared and tested. The voltammograms (Fig. S3C) shows the sensing responses of MIP/PC/GCE and NIP/PC/GCE toward LID. It can be observed that MIP/PC/GCE exhibits an apparent change in peak current ( $\Delta I = 19.6 \mu\text{A}$ ), whereas NIP/PC/GCE displays no obvious change ( $\Delta I = 1.6 \mu\text{A}$ ). The results confirm the existence of imprinting effect and the function of MIP film. The effect of scan rate of MIP/PC/GCE was investigated by CV (Fig. S3D). The absolute values of the oxidation peak currents increase linearly with the square root of scan rate in the range from 10 to 200  $\text{mV s}^{-1}$ , indicating that a diffusion-controlled electrochemical process at the sensor surface [9].

### Calibration curve and detection limit

Figure 3 shows the linear correlation between  $\Delta I$  and the logarithm of the concentration of LID ( $\ln C$ ). The corresponding linear regression equation is  $\Delta I (\mu\text{A}) = 4.1591 \ln C + 125.5321$  ( $R^2 = 0.9946$ ) in the range of  $2 \times 10^{-13} \sim 8 \times 10^{-9} \text{ M}$ , where current density is  $1.76 \mu\text{A}\cdot\text{cm}^{-2}$ , sensitivity is  $219.90 \mu\text{A}\cdot\mu\text{M}^{-1}\cdot\text{cm}^{-2}$  and limit of detection (LOD) is  $6.7 \times 10^{-14} \text{ M}$  ( $S/N = 3$ ). This is lower than the LOD of any other LID electrochemical method reported so far. This comparison is summarized in Table 1.

### Selectivity of LID-MIP/PC/GCE

In selectivity study, the concentration of LID and its structural analogues (BC, PC and MC) was set at  $6 \times 10^{-12} \text{ M}$ . Detection of these structural analogues was carried out individually. It

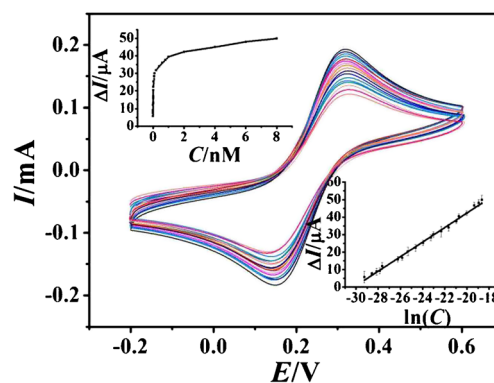


**Fig. 3** Cyclic voltammograms of MIP/PC/GCE after rebinding LID at 0.335 V in the concentration range of  $2 \times 10^{-13} \sim 8 \times 10^{-9} \text{ M}$  in 5 mM  $[\text{Fe}(\text{CN})_6]^{3-/4-}$  and 0.1 M  $\text{KNO}_3$  at the scan rate of  $100 \text{ mV s}^{-1}$ . The top-left inset shows the correlation between oxidation peak current shift and concentration of LID. The bottom-right inset is the calibration curve for LID detection correlating oxidation peak current shift with the logarithm of the concentration of LID

can be seen from Fig. 4 that MIP/PC/GCE has much higher response to LID than to the analogues, and the NIP electrode exhibits no obvious current difference in detecting all the analytes. *T*-test of the results further proves remarkable differences in the sensing response between LID and its analogues with a significant level of 0.01. These results confirm the importance of MIP film, which plays a role based on complementation between template and the imprinting sites in size, shape and functionality, whereas NIP/PC/GCE shows weak response due to lack of imprinting effect. Moreover, mixture of LID ( $6 \times 10^{-12} \text{ M}$ ) and interfering ions ( $\text{NH}_4^+$ ,  $\text{Na}^+$ ,  $\text{Ca}^{2+}$ ,  $\text{K}^+$ ,  $\text{NO}_3^-$ ,  $\text{Cl}^-$  and  $\text{SO}_4^{2-}$ ;  $6 \times 10^{-11} \text{ M}$ ) was analyzed. It was found that the sensing response from LID alone is 97.05% of the response from the mixture of LID and ions. This goes to show that the sensor possesses good selectivity in a complicated matrix even though the amount of interfering ions is remarkably higher than that of analyte.

### Repeatability and stability

LID at three different concentrations ( $2 \times 10^{-12}$ ,  $4 \times 10^{-12}$  and  $6 \times 10^{-12} \text{ M}$ ) were measured in triplicate using the same MIP/PC/GCE. Relative standard deviation (RSD) was less than 2.5%, which indicates the good repeatability of the sensor.

After each use, MIP/PC/GCE was stored at room temperature. No obvious change was found in response of LID ( $6 \times 10^{-12} \text{ M}$ ) in the first week. After one-month storage, the current response decreased by 3.1%, compared with the initial electrical signal, exhibiting decent stability of the hybrid electrode.

### Real sample analysis

To verify practicality and accuracy of the sensor in real sample detection, LID in rat serum was analyzed by MIP/PC/GCE

**Table 1** Comparison of the major characteristics of different electrochemical sensors in detecting LID

Electrodes	Linear range ( $\mu\text{M}$ )	LOD ( $\mu\text{M}$ )	RSD (%)	Ref.
CPE <sup>a</sup> /QD <sup>b</sup> -rGO <sup>c</sup>	2.55 ~ 14.4	0.95	–	[13]
Boron-doped diamond electrodes	24.2 ~ 114	42.67	2.3	[14]
MIP/Pt-PdNPs-NH <sub>2</sub> -MWCNT <sup>d</sup> /Pt-Pd NPs-PtNWs <sup>e</sup> /COOH-r-GO <sup>f</sup> /GCE	$5.0 \times 10^{-3}$ ~ 4.8	$1.0 \times 10^{-4}$	3.6	[16]
Au/MPA <sup>g</sup> /Hb <sup>h</sup> electrodes	0.5 ~ 2.9	0.29	–	[33]
MIP/PC/GCE	$2 \times 10^{-4}$ ~ 8	$6 \times 10^{-5}$	2.8	This work

<sup>a</sup> CPE: carbon paste electrode<sup>b</sup> QD: quantum dots<sup>c</sup> rGO: reduced graphene oxide<sup>d</sup> Pt-Pd NPs-NH<sub>2</sub>-MWCNT: Pt-Pd bimetallic nanoparticles and aminated multi-walled carbon nanotubes<sup>e</sup> Pt-Pd NPs-PtNWs: Pt-Pd bimetallic nanoparticles and porous Pt nano-networks<sup>f</sup> COOH-r-GO: carboxyl graphene<sup>g</sup> MPA: 3-mercaptopropionic acid<sup>h</sup> Hb: hemoglobin

through standard addition method. The analytical results (Table S2) show good accuracy with recovery values ranging from 97.9% to 105.0%. Furthermore, HPLC as a standard method was also employed to test LID in the same rat serum and the results were in good accordance with those from our sensor, reflecting the reliability of the sensor.

## Conclusion

The work describes a novel hybrid electrochemical sensor for highly selective and sensitive detection of LID. To our knowledge, this is the first report on PC-coated GCE with the combination of molecularly imprinted polymeric film as a promising hybrid sensor. Preparation of the sensor was conducted in a tender manner and integration of PC and MIP shows an excellent performance for detecting ultratrace level of LID. In

the composite modification membranes, the homogeneously dispersed PC provides considerable surface area which helps to accelerate electron transportation and expands the platform for MIP loading as well. Secondly, molecular imprinting technique is introduced to guarantee specific recognition toward LID. Utilization of the sensor in assaying LID takes much less time and effort than the common method of HPLC without losing accuracy. However, it should be mentioned that the incubation step during sensor detection needs at least 10 min, which impairs its convenience in practical application. Further work will be performed to decrease assay duration and make the whole strategy more facile and convenient. In conclusion, our work not only reports a fascinating porous carbon material and its application together with MIP in electrochemical detection field, but also suggests the favorable potential of PC in battery, electrocatalysis and supercapacitor.

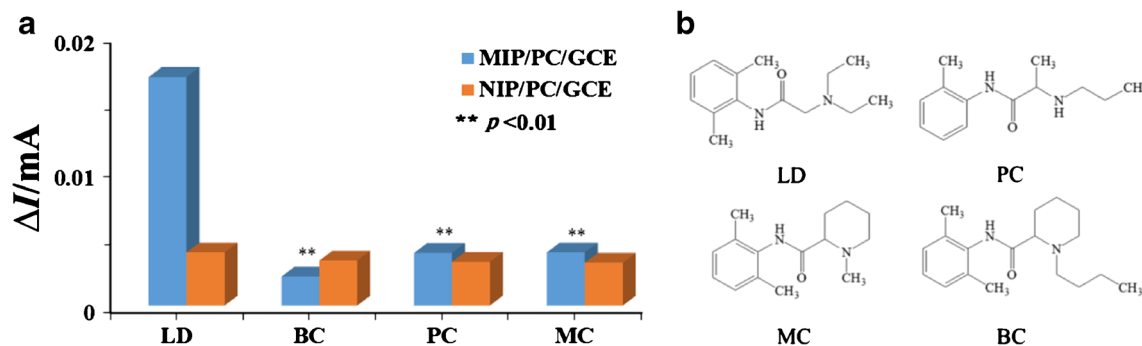


**Fig. 4** Comparison of sensor responses towards LID and its structural analogues at  $8 \times 10^{-12}$  M using MIP/PC/GCE and NIP/PC/GCE (**a**), and chemical structures of LID and the analogues (**b**)

**Acknowledgements** The project financially supported by National Natural Science Foundation of China (81460543, 81773680, 61671308).

**Compliance with ethical standards** The author(s) declare that they have no competing interests.

**Conflict of Interest** We abide by compliance with ethical standards during the animal experiment.

## References

- Ding SN, JJ X, Zhang WJ, Chen HY (2006) Tris(2,2'-bipyridyl)ruthenium(II)-zirconia-Nafion composite modified electrode applied as solid-state electrochemiluminescence detector on electrophoretic microchip for detection of pharmaceuticals of tramadol, lidocaine and ofloxacin. *Talanta* 70(3):572–577
- Marret E, Rolin M, Beaussier M, Bonnet F (2010) Meta-analysis of intravenous lidocaine and postoperative recovery after abdominal surgery †. *Br J Surg* 95(11):1331–1338
- Adcock JJ, Douglas GJ, Garabette M, Gascoigne M, Beatch G, Walker M, Page CP (2003) RSD931, a novel anti-tussive agent acting on airway sensory nerves. *Br Aust J Pharm* 138(3):407–416
- Porrà R, Berri S, Gagliardi L, Chimenti P, Granese A, Orsi DD, Carpani I, Tonelli D (2004) Development of an HPLC method for the identification and dosage of non-allowed substances in cosmetic products. Part I: local anaesthetics and antihistaminics. *Anal Bioanal Chem* 380(5–6):767–772
- Zargar B, Hatamie A (2014) Hollow fiber liquid based microextraction combined with high-performance liquid chromatography for the analysis of lidocaine in biological and pharmaceutical samples. *Anal Methods* 6(8):2506–2511
- Qin W, Jiao Z, Zhong M, Shi X, Zhang J, Li Z, Cui X (2010) Simultaneous determination of procaine, lidocaine, ropivacaine, tetracaine and bupivacaine in human plasma by high-performance liquid chromatography. *J Chromatogr B* 878(16):1185–1189
- Karlaganis G, Bircher J (1987) Bioavailability determination of lidocaine by capillary gas chromatography ammonia chemical ionization mass spectrometry. *Biol Mass Spectrom* 14(9):513
- Yamini Y, Seidi S, Feizbakhsh R, Baheri T, Rezazadeh M (2014) Liquid-phase microextraction based on two immiscible organic solvents followed by gas chromatography with mass spectrometry as an efficient method for the preconcentration and determination of cocaine, ketamine, and lidocaine in human urine samples. *J Sep Sci* 37(17):2364–2371
- Li YC, Zhang L, Liu J, Zhou SF, Al-Ghanem KA, Mahboob S, Ye BC, Zhang X (2016) A novel sensitive and selective electrochemical sensor based on molecularly imprinted polymer at nanoporous gold leaf modified electrode for warfarin sodium determination. *RSC Adv* 6(49):43724–43731
- Song H, Zhang L, Yu F, Ye BC, Li Y (2016) Molecularly imprinted polymer functionalized nanoporous Au-Ag alloy microrod: novel supportless electrochemical platform for ultrasensitive and selective sensing of metronidazole. *Electrochim Acta* 208:10–16
- Li Y, Liu J, Liu M, Yu F, Zhang L, Tang H, Ye BC, Lai L (2016) Fabrication of ultra-sensitive and selective dopamine electrochemical sensor based on molecularly imprinted polymer modified graphene@carbon nanotube foam. *Electrochem Commun* 64:42–45
- Huang B, Xiao L, Dong H, Zhang X, Wei G, Mahboob S, Al-Ghanim KA, Yuan Q, Li Y (2017) Electrochemical sensing platform based on molecularly imprinted polymer decorated N,S co-doped activated graphene for ultrasensitive and selective determination of cyclophosphamide. *Talanta* 164:601–607
- Matos CRS, Souza HO, Santana TBS, Luan PMC, Cunha FGC, Sussuchi EM, Gimenez IF (2017) Cd 1-x Mg x Te semiconductor nanocrystal alloys: synthesis, preparation of nanocomposites with graphene-based materials, and electrochemical detection of lidocaine and epinephrine. *Microchim Acta* 184(2):1–10
- Oliveira RTS, Salazar-Banda GR, Ferreira VS, Oliveira SC, Avaca LA (2010) Electroanalytical determination of Lidocaine in pharmaceutical preparations using boron-doped diamond electrodes. *Electroanalysis* 19(11):1189–1194
- Kachooangi RT, Wildgoose GG, Compton RG (2010) Using capsaicin modified multiwalled carbon nanotube based electrodes and p-Chloranil modified carbon paste electrodes for the determination of amines: application to benzocaine and Lidocaine. *Electroanalysis* 20(23):2495–2500
- Yang G, Zhao F (2014) A novel electrochemical sensor for the determination of lidocaine based on surface-imprinting on porous three-dimensional film. *J Mater Chem C* 2(47):10201–10208
- Niu M, Pham-Huy C, He H (2016) Core-shell nanoparticles coated with molecularly imprinted polymers: a review. *Microchim Acta* 183(10):2677–2695
- Li Y, Song H, Zhang L, Zuo P, Ye BC, Yao J, Chen W (2016) Supportless electrochemical sensor based on molecularly imprinted polymer modified nanoporous microrod for determination of dopamine at trace level. *Biosens Bioelectron* 78:308
- Xu J, Wang Y, Hu S (2016) Nanocomposites of graphene and graphene oxides: synthesis, molecular functionalization and application in electrochemical sensors and biosensors. A review. *Microchim Acta* 184(1):1–44
- Dai H, Xiao D, He H, Li H, Yuan D, Zhang C (2015) Synthesis and analytical applications of molecularly imprinted polymers on the surface of carbon nanotubes: a review. *Microchim Acta* 182(5–6):893–908
- Xiao L, Xu R, Yuan Q, Wang F (2017) Highly sensitive electrochemical sensor for chloramphenicol based on MOF derived exfoliated porous carbon. *Talanta* 167(5):39–43
- Shao Y, Wang J, Wu H, Liu J, Aksay IA, Lin Y (2010) Graphene based electrochemical sensors and biosensors: a review. *Electroanal* 22(10):1027–1036
- Li D, Jia J, Wang J (2010) Simultaneous determination of Cd(II) and Pb(II) by differential pulse anodic stripping voltammetry based on graphite nanofibers–Nafion composite modified bismuth film electrode. *Talanta* 83(2):332–336
- Chaikittisilp W, Ariga K, Yamauchi Y (2012) A new family of carbon materials: synthesis of MOF-derived nanoporous carbons and their promising applications. *J Mater Chem A* 1(1):14–19
- Xiao L, Zhou S, Hu G, Xu H, Wang Y, Yuan Q (2015) One-step synthesis of isoreticular metal-organic framework-8 derived hierarchical porous carbon and its application in differential pulse anodic stripping voltammetric determination of Pb(II). *RSC Adv* 5(94):77159–77167
- Wang L, Stuckert NR, Chen H, Yang RT (2011) Effects of Pt particle size on hydrogen storage on Pt-doped metal-organic framework IRMOF-8. *J Phys Chem C* 115(11):4793–4799
- Lavin-Lopez MP, Valverde JL, Sanchez-Silva L, Romero A (2016) Solvent-based exfoliation via sonication of graphitic materials for graphene manufacture. *Ind Eng Chem Res* 55(4):845–855
- Jiang HL, Liu B, Lan YQ, Kuratani K, Akita T, Shioyama H, Zong F, Xu Q (2011) From metal-organic framework to nanoporous carbon: toward a very high surface area and hydrogen uptake. *J Am Chem Soc* 133(31):11854

29. Yang LM, Ravindran P, Vajeeston P, Tilset M (2012) Properties of IRMOF-14 and its analogues M-IRMOF-14 (M = Cd, alkaline earth metals): electronic structure, structural stability, chemical bonding, and optical properties. *Phys Chem Chem Phys* 14(14):4713–4723
30. Mattevi C, Eda G, Agnoli S, Miller S, Mkhoyan KA, Celik O, Mastrogiovanni D, Granozzi G, Garfunkel E, Chhowalla M (2009) Evolution of electrical, chemical, and structural properties of transparent and conducting chemically derived Graphene thin films. *Adv Funct Mater* 19(16):2577–2583
31. Ou J, Zhang Y, Chen L, Zhao Q, Meng Y, Guo Y, Xiao D (2015) Nitrogen-rich porous carbon derived from biomass as a high performance anode material for lithium ion batteries. *J Mater Chem A* 3(12):6534–6541
32. Yang SJ, Kim T, Ji HI, Kim YS, Lee K, Jung H, Chong RP (2012) MOF-derived hierarchically porous carbon with exceptional porosity and hydrogen storage capacity. *Chem Mater* 24(3):464
33. Tan G, Bolat G, Onur MA, Abaci S (2012) Determination of lidocaine based on electrocatalysis of a chemically modified electrode. *Turk J Chem* 36(4):593–600